



HAL
open science

Neuroprotective effect of the alpha 7 nicotinic receptor agonist PHA 543613 in an in vivo excitotoxic adult rat model

Laura Foucault-Fruchard, Aurélie Doméné, Guylène Page, Marguerite Windsor, Patrick Emond, Nuno Rodrigues, Frédéric Dollé, Annelaure Damont, Frédéric Buron, Sylvain Routier, et al.

► To cite this version:

Laura Foucault-Fruchard, Aurélie Doméné, Guylène Page, Marguerite Windsor, Patrick Emond, et al.. Neuroprotective effect of the alpha 7 nicotinic receptor agonist PHA 543613 in an in vivo excitotoxic adult rat model. *Neuroscience*, 2017, 356, pp.52-63. 10.1016/j.neuroscience.2017.05.019 . hal-04483971

HAL Id: hal-04483971

<https://hal.science/hal-04483971>

Submitted on 4 Apr 2024

HAL is a multi-disciplinary open access archive for the deposit and dissemination of scientific research documents, whether they are published or not. The documents may come from teaching and research institutions in France or abroad, or from public or private research centers.

L'archive ouverte pluridisciplinaire **HAL**, est destinée au dépôt et à la diffusion de documents scientifiques de niveau recherche, publiés ou non, émanant des établissements d'enseignement et de recherche français ou étrangers, des laboratoires publics ou privés.

NOTICE: This is the accepted author manuscript of the publication

Neuroprotective effect of the alpha 7 nicotinic receptor agonist PHA 543613 in an *in-vivo* excitotoxic adult rat model

Laura Foucault-Fruchard, Aurélie Doméné, Marguerite Windsor, Patrick Emond, Nuno Rodrigues, Frédéric Dollé, Anne Laure Damont, Frédéric Buron, Sylvain Routier, Sylvie Chalon, Daniel Antier.

Published in Neuroscience

doi: 10.1016/j.neuroscience.2017.05.019

Available online 18 May 2017

Direct link to the final version of the article:

[10.1016/j.neuroscience.2017.05.019](https://doi.org/10.1016/j.neuroscience.2017.05.019)

<http://www.sciencedirect.com/science/article/pii/S0306452217303445>

© <2017>. This manuscript version is made available under the CC-BY-NC-ND 4.0 license
<http://creativecommons.org/licenses/by-nc-nd/4.0/>

1 **Neuroprotective effect of the alpha 7 nicotinic receptor agonist PHA 543613 in an *in-***
2 ***vivo* excitotoxic adult rat model**

3

4 Laura Foucault-Fruchard^{1,2,*}, Aurélie Doméné¹, Marguerite Windsor², Patrick Emond¹, Nuno
5 Rodrigues³, Frédéric Dollé⁴, Anne Laure Damont⁴, Frédéric Buron³, Sylvain Routier³, Sylvie
6 Chalon^{1,§}, Daniel Antier^{1,2,§}.

7 [§]Contributed equally

8 ¹UMR INSERM U930, Université François Rabelais, Tours, France

9 ²CHRU de Tours, Hôpital Bretonneau, Tours, France

10 ³UMR CNRS 7311, Institut de Chimie Organique et Analytique, Université d'Orléans,
11 Orléans, France

12 ⁴CEA, I2BM, Service Hospitalier Frédéric Joliot, Orsay, France

13

14 Email addresses:

15 laura.foucault@univ-tours.fr

16 aurelie.domene@univ-tours.fr

17 marguerite.windsor-2@etu.univ-tours.fr

18 patrick.emond@univ-tours.fr

19 nuno.rodrigues@univ-orleans.fr

20 Frederic.DOLLE@cea.fr

21 annelaure.damont@cea.fr

22 frederic.buron@univ-orleans.fr

23 sylvain.routier@univ-orleans.fr

24 sylvie.chalon@univ-tours.fr

25 daniel.antier@univ-tours.fr

26

27

28

29 *Corresponding author: Laura Foucault-Fruchard

30 UMR INSERM U930

31 UFR de Médecine,

32 10 Boulevard Tonnellé,

33 Tours 37032, France

34 laura.foucault@univ-tours.fr

35

36 **Abstract**

37 **Background**

38 Neuroinflammation is a key-component of the pathophysiology of neurodegenerative
39 diseases and its regulation, a major therapeutic target to reach since no efficient curative
40 treatment is available. The link between nicotine intake and positive outcome in
41 neurodegenerative diseases has been established suggesting a role played by nicotinic
42 receptors especially the nicotinic acetylcholine receptors $\alpha 7$ ($\alpha 7nAChRs$). The objective of
43 this study was to evaluate *in vivo* the potential dose effects of the PHA 543613, a high affinity
44 agonist of $\alpha 7nAChRs$, on neuron survival and striatal neuroinflammation especially using a
45 radioligand never studied in rat model of brain excitotoxic.

46

47 **Methods**

48 Twenty-six adult male Wistar rats were lesioned in the right striatum with quinolinic acid (QA)
49 and received either vehicle (Sham group; n=8) or PHA 543613 at a concentration of 6 mg/kg
50 (QA-PHA6; n=8) or 12 mg/kg (QA-PHA12; n=10) intra-peritoneally 1 h before QA lesioning
51 and then twice a day until sacrifice at day-4 post-lesion. The measured kinetic parameters of
52 PHA 543613 in rats were taken into account when the administration schedule was
53 established. A first study compared TSPO quantitative autoradiography in QA-lesioned
54 brains with [3H]DPA-714 and [3H]PK11195 (n=9). The effects of the PHA 543613 on
55 microglia activation and neuronal survival have then been evaluated through [3H]DPA-714
56 binding and immunofluorescence staining (Ox-42, NeuN) on adjacent brain sections.

57 **Results**

58 We demonstrated that [³H]DPA-714 provide a better signal-to-noise ratio than [³H]PK11195.

59 In addition, we showed that chronic PHA 543613 treatment administered at a dose of
60 12mg/kg to QA-lesioned rats significantly protected neurons and reduced the intensity of
61 neuroinflammation measured by TSPO and Ox-42 immunostaining.

62

63 **Conclusions**

64 This study, among the first to evaluate the effects of an $\alpha 7$ nAChRs agonist treatment in an
65 excitotoxic model of neuroinflammation with [³H]DPA-714, indicates that PHA 543613 exerts
66 neuroprotective effects on the striatal neurons associated with a reduction in microglial
67 activation. This reinforces the hypothesis that $\alpha 7$ nAChRs agonist can provide beneficial
68 effects in the treatment of patients with neurodegenerative diseases through modulation of
69 neuroinflammation.

70

71 **Keywords**

72 Nicotinic acetylcholine receptors $\alpha 7$ - PHA 543613 - TSPO – Neuroinflammation - DPA-714 -
73 PK-11195 – autoradiography – immunofluorescence – Neurodegeneration

74

75

76

77

78

79

80

81

82

83

84

85 **Background**

86 Neuroinflammation is a reaction of the central nervous system in response to infection, injury
87 or trauma. This is a physiological component of innate immunity, which involves a non-
88 specific and early response against a pathogen in order to neutralize and minimize damage
89 at the neuronal level by repairing damaged brain tissue. Microglia-driven neuroinflammation
90 has a beneficial effect on scavenging cell debris, tissue healing and repair. However, during
91 chronic neuroinflammation, activated microglial cells produce pro-inflammatory cytokines,
92 reactive oxygen species and derivatives of nitric oxide (NO) [1]. This activity is responsible
93 for neuronal death by apoptosis which in turn stimulates microglial activation that contributes
94 to the pathophysiology of neurodegenerative diseases [2,3]. Neurons are also able to
95 produce proinflammatory cytokines, complement factors and derivatives of NO. These
96 inflammatory mediators can cause neuronal dysfunction and cell death [4,5].

97 Neuroinflammation is well known as an important element of brain disorders and in particular
98 neurodegenerative diseases [6].

99 Regulating neuroinflammation represents therefore a major challenge in the management of
100 patients affected by neurodegenerative diseases such as Alzheimer's, Parkinson's or
101 Huntington's diseases. Nowadays, only symptomatic treatments are available and no
102 curative treatment has a marketing authorization for neurodegenerative diseases. Several
103 lines of research on an anti-inflammatory therapeutic approach have been explored in animal
104 models and in humans, but were all unsuccessful [7–11]. Epidemiological studies have
105 shown that smokers have a lower risk of neurodegenerative diseases than the rest of the
106 population [12–15]. These observations led to an interest in nicotine administration which, by
107 binding to nicotinic acetylcholine receptors, may have beneficial effects on the symptoms of
108 neurodegenerative diseases, particularly Parkinson's disease (PD) [16–20].

109 Among the different subtypes of nicotinic receptors, the $\alpha 7$ ($\alpha 7$ nAChRs) are highly expressed
110 in the mammalian brain particularly by neurons and glial cells [21–23]. They belong to the
111 family of ligand-gated ion channels and have a homopentameric structure of five $\alpha 7$ subunits.
112 $\alpha 7$ nAChRs are involved in the control of voluntary movement, memory and attention, sleep

113 and waking and pain and anxiety. They appear to be involved in a number of brain disorders
114 such as drug addiction, schizophrenia and neurodegenerative diseases like Alzheimer's
115 disease (AD) and PD [21]. It has been shown that $\alpha 7$ nAChRs activation improved cognitive
116 functions in several animal models that mimic AD, and the $\alpha 7$ nAChRs agonist, EVP-6124, is
117 currently in clinical phase III in mild to moderate AD patients [24]. Additionally, several
118 $\alpha 7$ nAChRs agonists are being evaluated for the treatment of PD [25]. First results support
119 the idea that drugs acting at $\alpha 7$ nAChRs may be beneficial including one study demonstrating
120 the role of $\alpha 7$ nAChRs agonists for the reduction of L-dopa-induced dyskinesias [26-28]. In
121 addition, PNU 282987 and PHA 543613 $\alpha 7$ nAChRs agonists have demonstrated
122 neuroprotective and anti-inflammatory effects in different intracerebral haemorrhage models
123 [29,30]. Moreover, these 2 agonists and PNU 120596, an $\alpha 7$ nAChRs positive allosteric
124 modulator, have proved the same effect in both *in-vitro* and *in vivo* brain ischemia models
125 [31]. The modulation of the $\alpha 7$ nAChRs activation in macrophages influences the synthesis of
126 pro-inflammatory cytokines involved in the regulation of the "cholinergic anti-inflammatory
127 pathway" [32].

128

129 PHA 543613 [N- (3R) -1-azabicyclo [2.2.2] - Oct-3- yl- furo [2,3 -c] pyridine -5-carboxamide
130 hydrochloride] is a selective agonist of $\alpha 7$ nAChRs, known for its high affinity for $\alpha 7$ nAChRs
131 [33,34]. Studies have reported a significant anti-inflammatory effect on primary cultures of
132 neurons and astrocytes (unpublished observations, G. Page). *In vivo*, it improved recognition
133 memory in an AD mouse model [35]. Moreover, promising effects on cognitive function were
134 also observed in a schizophrenia' disease model [33]. Recent study has also demonstrated
135 that PHA 543613 exerts neuroprotective effects on the striatal dopaminergic neurons with a
136 reduction in microglial activation in a PD rat model [28]. Thus, data published in literature
137 relate that therapies targeting glial cells, and more precisely the agonists of $\alpha 7$ nAChRs,
138 might provide benefit in neurodegenerative disorders [36]. However, the interactions between
139 the neuroprotective and anti-inflammatory effects are not clearly elucidated. Regarding this
140 question, we used a rat model of acute neuroinflammation obtained by unilateral striatal

141 injection of quinolinic acid (QA) in which we evaluated the effects of a chronic administration
142 of PHA 543613. QA is a strong agonist of glutamate NMDA (N-methyl-D-aspartate)
143 receptors. Overactivation of NMDA receptors causes a massive intracellular influx of calcium
144 that leads to neuronal death by activation of various enzymes triggering different cell
145 components then leading to neuronal death [37]. Factors released during the death of these
146 neurons rapidly leads to significant microglial activation. This model of Huntington's disease
147 has recently been shown to be useful in studying the overexpression of the translocator
148 protein (TSPO), a marker of neuroinflammation [38-40]. Therefore, the main purpose of the
149 present study was to evaluate *in vivo* the potential dose effects of the selective agonist of
150 $\alpha 7$ nAChRs, PHA 543613, on both neuronal survival and microglial activation in a
151 neuroinflammatory excitotoxic rat model using QA intrastriatal injection. We also interested in
152 the effects of repeated administration of PHA 543613 on $\alpha 7$ nAChRs density in our rat model
153 of brain excitotoxic. As a secondary goal, the study aimed to carry out autoradiographic
154 quantification of TSPO expression with a radioligand never studied in a rat model of
155 neuroinflammation: the [³H]DPA-714 [41].

156

157 **Materials and Methods**

158 **Animals**

159 All procedures were conducted in accordance with the European Community Council
160 Directive 2010/63/EU for laboratory animal care and the experimental protocol was validated
161 by the Regional Ethical Committee (Authorization N°2015022011523044). Experiments were
162 carried out on 10-week-old normotensive male Wistar rats (CERJ, France) weighing 290–
163 300g at the beginning of experiments. Animals were housed in groups of 2 per cage in a
164 temperature (21 ± 1°C) and humidity (55 ± 5%) controlled environment under a 12-h
165 light/dark cycle, with food and water available *ad libitum*. A total of 39 animals were used for
166 the experiments described below.

167

168

169 **Excitotoxic neuroinflammation model**

170 For unilateral striatal QA lesion, rats (n=35) were anaesthetized with isoflurane (Aerrane™,
171 Baxter, France; 4% for induction and 2% for maintenance) and placed in a stereotaxic David
172 Kopf apparatus (tooth bar: -3.3 mm). The animals' body temperature ($36.9 \pm 0.6^\circ\text{C}$) was
173 monitored during the surgery by using a thermal probe. The animals were unilaterally
174 injected with 150 nmol of QA (Sigma-Aldrich, Lyon, France), dissolved in 0.1 mol/L
175 phosphate-buffered saline (PBS) pH 7.4, into the right striatum (injection rate: 0.5 $\mu\text{L}/\text{min}$)
176 using a 25 μL microsyringe (Hamilton, Bonaduz, Switzerland) and a micropump (KD
177 Scientific, Holliston, Massachusetts, USA). QA (2 μL) was injected at the following
178 coordinates: AP: + 0.7 mm; ML: - 3 mm; DV: - 5.5 mm from bregma according to Paxinos
179 and Watson [42]. The injection syringe was left in place for an additional 4 min to avoid QA
180 back-flow, and then slowly removed. After surgery, the scalp was sutured and the rats were
181 given buprenorphine (0.05 mg/kg sub-cutaneously) for postoperative pain.

182

183 **Comparative evaluation of TSPO radioligands [³H]DPA-714 and [³H]PK-11195 by**
184 **autoradiographic study in QA lesioned rats**

185 We first measured the *in vitro* binding of TSPO by [³H]DPA-714 in comparison to [³H]PK-
186 11195 in adjacent brain sections from 9 QA-lesioned rats. [³H]DPA-714 was prepared
187 according to *Damont and al, 2015* [41] (specific activity 2.1 GBq/ μmol) and [³H]PK-11195
188 was commercially purchased (specific activity 3.06 GBq/ μmol ; Perkin Elmer, Norwalk, CT,
189 USA). Autoradiographic studies were performed 7 days after QA lesion. After decapitation
190 under isoflurane anesthesia, the brains were carefully removed on ice, then frozen in
191 isopentane cooled at -35°C and stored at -80°C until use. Coronal brain sections 16 μm thick
192 were cut with a cryostat (CM 3050S™, Leica, Germany) at -20°C , collected on gelatinized
193 slides and stored at -80°C for at least 4 days. Brain sections were allowed to equilibrate at
194 room temperature (RT) for 3h, then incubated with 1 nmol/L of labelled ligand ([³H]DPA-714
195 or [³H]PK-11195) in 50 mmol/L Tris-HCl buffer pH 7.4 at RT for 60 min. Non-specific binding
196 was assessed in the presence of 1 $\mu\text{mol}/\text{L}$ stable PK-11195 (Sigma Aldrich, Lyon, France).

197 Sections were rinsed twice in ice cold buffer (4°C) for 5 min, then briefly in distilled water at
198 4°C and dried at RT. Dry sections were made conductive by an application of metal electric
199 tape (3M™, Euromedex, Souffelweyersheim, France) on the other side and then placed in
200 the gas chamber of the β-imager™ 2000 (Biospace Lab, Paris, France). Acquisitions were
201 collected over a period of 4 h. Two anatomical regions of interest (ROIs), i.e., the ipsi-lateral
202 (IL) and contra-lateral (CL) striata were selected and identified in Paxinos and Watson atlas
203 [42]. Using the β-vision software (Biospace Lab, Paris, France), the level of bound
204 radioactivity was directly determined by counting the number of β-particles emitted from the
205 delineated area. The radioligand signal in the ROIs was measured for 6 sections per brain
206 and expressed as counts per minute per square millimeter (cpm/mm²). Specific binding was
207 determined by subtracting non-specific binding from total binding. Radioactivity was
208 quantified using an image analyzer (M3-vision™ Biospace Instruments, Paris, France).
209 The percentage increase of TSPO binding in IL *versus* (vs) CL hemisphere was calculated
210 as :
$$\frac{IL-CL}{CL} \times 100$$

211

212

213 **Pharmacokinetics of PHA 543613**

214 Given the lack of data on the pharmacokinetics of PHA 543613, a study to determine the
215 evolution of the concentration vs time in plasma and in brain was performed to choose the
216 most suitable dosing regimen and to confirm the PHA 543613 cerebral diffusion. PHA
217 543613 concentration was measured with ultra liquid chromatography (UHPLC UltiMate®
218 3000 system, Thermo Scientific Dionex™, Villebon-sur-Yvette, France) coupled with high
219 resolution mass spectrometry (Orbitrap Q exactive™, Thermo Scientific™, Villebon-sur-
220 Yvette, France) in the serum and brain of 4 treated rats after one i.p injection of PHA 543613
221 at a dose of 6 mg/kg. Blood samples from the jugular vein were collected at 0.5, 1, 3, 6 and
222 24 h post injection in heparinized tubes. Blood was centrifuged at 2,000 g, for 20 min at 4°C,
223 plasma was removed and then kept at -20°C. The rats were killed by decapitation under
224 isoflurane anesthesia. The whole brain was quickly removed and striatum removed and kept

225 at -80°C. Striatum and plasma were homogenized respectively in 2 mL and 400 µL of ethyl
226 acetate with internal standard (PHA 568487, Tocris Bioscience, Bristol, UK, 1 µg/mL) and
227 centrifuged at 15,000 g, for 5 min at 4°C. Supernatants were removed; ethyl acetate was
228 evaporated. They were filtered and injected into the liquid chromatograph (C18
229 chromatography). A multistep gradient (followed by a 2 min equilibration time) had a mobile
230 phase A of 0.5% formic acid in water and a mobile phase B of ACN acidified with 0.5%
231 formic acid; the gradient operated at a flow rate of 0.3 mL/min over a run time of 7.5 min. The
232 acquisition and data processing was performed with X-calibur 2.2 (Thermo Scientific™,
233 Villebon-sur-Yvette, France).

234

235 **Experimental procedure and drug treatment**

236 PHA 543613 hydrochloride (ICOA, Orléans, France) was dissolved in sterile water and intra-
237 peritoneally injected at a concentration of 6 or 12 mg/kg (300 µL/300 g body weight) 1 h
238 before QA lesioning and then twice a day every day until sacrifice at day 4 post-lesion.
239 Twenty six rats were included in this study and separated into 3 groups as follows: 10
240 lesioned rats received the treatment at 12 mg/kg (QA-PHA12 group), 8 rats received the
241 treatment at 6 mg/kg (QA-PHA6 group) and 8 lesioned rats received intra-peritoneal (i.p)
242 injection of vehicle according to the same administration schedule (Sham group).

243

244 **Evaluation of PHA 543613 dose-effect on neuroinflammation using TSPO**

245 **quantification by autoradiography**

246 First we investigated the potential dose-related effect of chronic 4-day treatment with PHA
247 543613 on striatum expression levels of TSPO. Rodents received either vehicle (n=5) or
248 PHA 543613 at 6 mg/kg (n=8) or 12 mg/kg (n=9) twice a day. In agreement with results
249 previously obtained (see section 3), the density of TSPO binding sites was measured by *in*
250 *vitro* autoradiographic experiment using [³H]DPA-714 (specific activity 2.1 TBq/mmol ; CEA ;
251 Orsay ; France) as described above. A total of 6 sections per brain were analyzed for each
252 rat. Data from brain sections were collected over 4h with the β-imager™ 2000. Specific

253 binding (expressed in cpm/mm²) from 2 ROIs, i.e., IL and CL striatum were determined.
254 Finally, the percentage increase of TSPO binding in IL vs CL hemisphere was calculated as :

$$\frac{\text{IL-CL} \times 100}{\text{CL}}$$

257

258 **Evaluation of PHA 543613 dose-effect on α 7nAChRs expression by autoradiography**

259 The density of α 7nAChRs binding sites was measured by *in vitro* autoradiography using
260 [¹²⁵I] α -bungarotoxin (specific activity 81.4 TBq/mmol; Perkin Elmer, Skovlunde, Denmark) on
261 brain sections adjacent to those used in the previous study, in Sham (n=6), QA-PHA6 (n=6)
262 and QA-PHA12 (n=6) rats. Brain sections were allowed to equilibrate at RT for 3h and then
263 were incubated with 0.4 nmol/L of [¹²⁵I] α -bungarotoxin in 50 mmol/L Tris-HCl buffer pH 7.4 at
264 RT for 60 min. Non-specific binding was assessed in the presence of 1 μ mol/L stable α -
265 bungarotoxin (Tocris Bioscience, Bristol, UK). The density of α 7nAChRs binding sites was
266 measured as described above (see section 3). A total of 6 sections per brain were analyzed
267 for each rat. Data from brain sections were collected over 4h with the β -imager™ 2000.
268 Specific binding (expressed in cpm/mm²) from 2 ROIs, i.e., IL and CL striatum was
269 determined.

270

271 **Evaluation of PHA effects on microglia activation and neuronal survival by** 272 **immunofluorescence**

273 Immunofluorescence measurements were performed on rats treated by PHA 543613 12
274 mg/kg (n=6) or vehicle (n=6). Coronal sections (16 μ m thick) of striatum adjacent to those
275 used for the autoradiographic study were used for the immunofluorescence staining of
276 neurons (NeuN, MAB377, Millipore, Molsheim, France) and activated microglia (Ox-42,
277 CBL1512, Chemicon International, Temecula, CA, USA). Slices were fixed in 4%
278 paraformaldehyde solution (Sigma, St Quentin Fallavier, France) at RT for 30 min. Tissue
279 sections were washed 3 times in PBS 0.1 mol/L for 5 min at RT and were then incubated for
280 3 h at RT in a buffer to enhance cell permeability and to block non-specific sites (PBS 0.1

281 mol/L/0,3%, Triton X-100/5%, normal goat serum). The sections were delineated using the
282 Dako Pen pencil (Z0334 ; Dako, Les Ulis, France) on the glass slide before incubation
283 overnight at 4°C with monoclonal mouse anti-NeuN (1:200) or monoclonal mouse anti-Ox-42
284 (1:100). Primary antibodies were diluted in PBS 0.1 mol/L/0.3% Triton X-100/1% normal goat
285 serum. After 3 washes with PBS 0.1 mol/L at RT for 5 min, sections were incubated for 1h in
286 a dark box at RT with goat anti-mouse DyLight™ 488 (KPL, Eurobio, Courtaboeuf, France) at
287 1:500 diluted in PBS/0.3% triton X-100/1% normal goat serum. The slices were washed twice
288 with PBS 0.1 mol/L and twice with distilled water. Then, they were incubated with 4'-6-
289 diamidino-2-phenylindole (DAPI) (0.1 µg/mL) for 15 min. After 3 washings in distilled water,
290 the slices were mounted with fluorescent mounting medium (S3023, DakoCytomation,
291 Trappes, France) and kept at 4°C until observation. Images were acquired with Morpho
292 Strider software (Explora-Nova™, La Rochelle, France) on Leica DM 5500B microscope.
293 Neurons and activated microglia cells were counted with Image J software (Rasband, WS,
294 Image J, US National Institute of Health, Bethesda, Maryland, USA) in 3 areas per striatum
295 for each section and in 2 sections per rat in order to obtain a representative sample of the
296 whole striatum. The number of cells was determined for each rat by calculating the average
297 obtained on the 6 analyzed areas for each hemisphere. Counting was performed by 2
298 independent operators. The percentage of neuronal loss and of increase of activated
299 microglia in ipsi- vs contra-lateral hemisphere were calculated as follows: $\frac{IL-CL}{CL} \times 100$
300

301 **Statistical Analysis**

302 Results were expressed as mean ± standard error of the mean (SEM). Correlation between
303 the specific binding of TSPO by [³H]PK-11195 and by [³H]DPA-714 was estimated by a two-
304 tailed Spearman test. To compare 2 groups of rats (PHA vs Sham), a Mann-Whitney test
305 was used. Comparisons between the binding in the IL and CL sides were performed using
306 the Wilcoxon one-tailed test. The level of significance was p<0.05 (GraphPad Prism software
307 version 5, San Diego, CA, USA).

308

309 **Results**

310 **Animals**

311 No physiological issues and no difference in body weight were observed between animals in
312 the Sham, QA-PHA6 and QA-PHA12 groups (on the day of lesion: 300 ± 20 g, 291 ± 4 g and
313 283 ± 4 g, respectively; at day-4 post-lesion: 278 ± 9 g, 282 ± 2 g and 268 ± 9 g,
314 respectively). Two rats, 1 in the Sham group and 1 in QA-PHA12 group, died on the lesion
315 day.

316

317 **PHA 543613 quantitative analysis with UHPLC coupled with high resolution mass**
318 **spectrometry**

319 One hour post-administration of PHA 543613 (6 mg/kg), a peak concentration was observed
320 in serum. Then, the concentration of PHA 543613 rapidly decreased. The rate of PHA
321 543613 in rat blood decreased by $35 \pm 7\%$ and $90 \pm 4\%$ at 2h and 6h post-i.p injection,
322 respectively. At 24h post-administration, PHA 543613 was no longer detectable in serum but
323 was present within striatum. Based on this observation, the rats were treated twice a day at a
324 dose of 6 or 12 mg/kg during the 4 days post-lesion. The first injection was carried out 1h
325 pre-lesion.

326

327 **Comparative evaluation of TSPO using [³H]DPA-714 and [³H]PK-11195**

328 The comparison of specific binding of TSPO between [³H]PK-11195 and [³H]DPA-714 by
329 autoradiography was performed on brain sections of rats sacrificed 7 days after intrastriatal
330 injection of QA (Fig. 1). Quantification of the autoradiography revealed that the binding of
331 TSPO either by [³H]PK-11195 or [³H]DPA-714 was significantly ($p < 0.05$) higher in the IL than
332 in the CL striatum. Non-specific binding in the CL or IL striatum assessed with $1 \mu\text{mol/L}$
333 PK11195, was lower with [³H]DPA-714 than with [³H]PK-11195, indicating a better signal-to-
334 noise for [³H]DPA-714 (0.06 ± 0.10 cpm/mm² vs 0.29 ± 0.02 cpm/mm² in CL respectively,
335 $p < 0.05$; 0.14 ± 0.02 cpm/mm² vs 0.37 ± 0.02 cpm/mm² in IL respectively; $p < 0.05$) (Fig. 1A).

336 Furthermore, the percentage increase of TSPO specific binding in IL vs CL striatum was
337 significantly ($p < 0.05$) higher for [^3H]DPA-714 than for [^3H]PK-11195 (821 ± 70 vs $489 \pm 42\%$
338 respectively) (Fig. 1B). In addition, the percentage increase of TSPO binding in IL vs CL
339 striatum was positively correlated using [^3H]DPA-714 and [^3H]PK-11195 (Fig. 1B, $\rho =$
340 0.9328 , $p < 0.05$).

341

342 **Evaluation of PHA 543613 dose-effect relationship on neuroinflammation using** 343 **autoradiography**

344 The TSPO density was evaluated on adjacent brain sections using [^3H]DPA-714 binding in
345 the IL and CL striatum from each rat in the Sham group and both PHA groups (6 mg/kg and
346 12 mg/kg) (Fig. 2A). The percentage increase of TSPO binding in IL vs CL striatum (Figure
347 2B) was lower in the QA-PHA6 group than in the Sham group but was not statistically
348 different ($764 \pm 72\%$ vs $967 \pm 64\%$, respectively). However, the percentage increase of TSPO
349 binding in IL vs CL striatum was significantly lower in the QA-PHA12 group ($731 \pm 34\%$ vs
350 $967 \pm 64\%$, respectively, $p < 0.05$). Finally, the increased rate of TSPO was higher but not
351 statistically different in QA-PHA6 and QA-PHA12 groups.

352

353 **Evaluation of PHA dose-effect on $\alpha 7\text{nAChRs}$ expression using autoradiography**

354 The $\alpha 7\text{nAChRs}$ expression was evaluated on adjacent brain sections by [^{125}I] α -bungarotoxin
355 binding in the IL and CL striatum from each rat in the Sham, QA-PHA6 and QA-PHA12
356 groups (Fig. 3A). The specific binding of [^{125}I] α -bungarotoxin (Fig. 3B) in the CL side on the
357 one hand and in IL side in the other hand were not significantly different between the Sham,
358 QA-PHA6 and QA-PHA12 groups (1.65 ± 0.42 , 1.60 ± 0.26 , and 1.83 ± 0.25 cpm/mm² in CL,
359 respectively; 1.36 ± 0.42 , 1.11 ± 0.18 , and 0.83 ± 0.27 cpm/mm² in IL, respectively).

360

361 **Evaluation of PHA 543613 effect on neuroinflammation by immunofluorescence**

362 The activated microglia were evaluated on adjacent brain sections by Ox-42 marker in the
363 CL and IL striatum in the Sham ($n = 6$) and QA-PHA12 ($n = 6$) groups (Fig. 4A and 4B). In both

364 groups, Ox-42 staining in IL striatum was significantly ($p < 0.05$) increased when compared to
365 CL striatum (Sham: 150 ± 13 cells stained in the IL vs 22 ± 2 in the CL side; QA-PHA12: 112
366 ± 5 cells stained in the IL vs 18 ± 1 in the CL side, $p < 0.05$) (Fig. 4C). Activated microglia (Ox-
367 42 positive cells) in IL striatum of QA-PHA12 rats were significantly lower (-34% , $p < 0.05$)
368 than in Sham. Moreover, activated microglia in IL vs CL were lower in the PHA12 group than
369 in Sham (531 ± 107 vs 609 ± 77 , respectively) (Fig. 4D).

370

371 **Evaluation of PHA 543613 on neuronal survival by immunofluorescence**

372 Neuron counting was performed on the same rats as above by using NeuN marker (Fig. 5A
373 and 5B). In both groups, NeuN staining was significantly decreased in IL vs CL side (QA-
374 PHA12: 114 ± 9 vs 206 ± 11 cells in the CL side, $p < 0.05$; Sham group: 59 ± 13 vs 184 ± 11
375 cells in the CL side, $p < 0.05$) (Fig. 5C). The number of neurons in IL side was 93% higher in
376 the QA-PHA12 group than in the Sham group ($p < 0.05$). Moreover, the neuronal loss in IL vs
377 CL striatum was significantly lower in the PHA12 than in the Sham group (44.5 ± 4 and $68 \pm$
378 7 , respectively, $p < 0.05$) (Fig. 4D).

379

380 **Discussion**

381 Neurodegenerative diseases are a major public health problem. Available treatments are
382 only able to improve symptoms, but are unable to slow down or stop the progression of the
383 disease. Many efforts are being deployed for developing such disease-modifying strategies
384 with agents able to have neuroprotective and/or neurorestorative effects. Several studies
385 suggest that neurodegeneration occurs in part because the environment is affected cascade
386 fashion during disease in a cell-autonomous process affecting neurons. This process, called
387 neuroinflammation, is defined by the contributions of glial cells, elements of the blood brain
388 barrier (BBB) or systemic inflammatory processes that can increase the severity of
389 neurodegenerative disease [36]. Thus, these observations indicate that therapies targeting
390 glial cells might provide beneficial effects on neurodegenerative disorders. Downregulation of
391 the activation of microglia can be obtained through the activation of $\alpha 7$ nAChRs localized on

392 microglial cells [43]. The agonists of $\alpha 7$ nAChRs have been the subjects of several studies on
393 schizophrenia but little data on the treatment of neurodegenerative diseases is published
394 nowadays [44]. Agonists of $\alpha 7$ nAChRs appear to be more efficient than acetylcholine at
395 inhibiting the inflammatory signalling and production of pro-inflammatory cytokines from
396 immune cells [45]. However, the effects induced by $\alpha 7$ nAChRs stimulation in traumatic brain
397 injury models appear to be either neuroprotective or toxic, highlighting the complexity of the
398 process.

399

400 The present study aimed to improve our knowledge relating to these potential therapeutic
401 targets by evaluating *in vivo* the effects of the selective $\alpha 7$ nAChRs agonist PHA 543613, on
402 both neuronal survival and microglial activation in a rodent model of excitotoxic
403 neuroinflammation based on striatal QA injection [39]. PHA 543613 was selected because
404 this compound has already demonstrated neuroprotective and anti-inflammatory effects in
405 different intracerebral haemorrhage models [29,30] and a recent study demonstrated that
406 PHA 543513 exerts neuroprotective effects on the striatal dopaminergic neurons with a
407 reduction in microglial activation in a Parkinson's disease rat model induced by 6-
408 hydroxydopamine (6-OHDA) lesion [28]. A preliminary study allowed us to confirm the ability
409 of this $\alpha 7$ nAChRs agonist to pass through the BBB and particularly to evaluate its
410 degradation half-life in order to optimize the drug administration schedule. Therefore, PHA
411 543613 was intra-peritoneally injected 1h before QA lesioning and then twice per day at days
412 1, 2, 3 and 4 post-lesion. The 4-day treatment duration was motivated by recently published
413 data reporting that quick tissue inflammation reached its highest level between day-4 to 7
414 post-QA lesion in this model based on the studied neuroinflammation markers [40,46]. The
415 unilateral intrastriatal injection of QA is admitted as an animal model mimicking the early
416 stages of Huntington's disease. It reproduces some biochemical, behavioural and pathologic
417 features of the disease in rodents and non-human primates [38,47,48]. QA is an endogenous
418 NMDA receptor agonist with excitotoxic properties which is found in normal subjects as a by-
419 product along the kynurenine pathway leading to the synthesis of the essential co-factors

420 nicotinic acid and nicotinamide adenine dinucleotide [49]. QA spares aspiny striatal
421 interneurons relative to spiny projection neurons [38]. In fact, it acts as a neurotoxin and
422 gliotoxin pro-inflammatory mediator and a pro-oxidant molecule that can alter BBB integrity
423 [50]. Dysfunction of neuronal activity consecutive to the QA injection can induce a pro-
424 inflammatory environment leading to the activation of surrounding microglial cells and in
425 consequence microglial activation. In the chosen excitotoxic model of neuroinflammation, the
426 excessive excitation of NMDA receptors leads to a massive intracellular influx of calcium.
427 This increase is associated with a mitochondrial dysfunction characterized by a decrease of
428 ATP levels that involves the formation and release of reactive oxygen and nitrogen species,
429 thus inducing cell oxidative damage as part of the degenerative process [51]. Moreover, the
430 activation of various enzymes (proteases, lipases and endonucleases) triggering different cell
431 components is also involved in neuronal death [37].

432

433 This *in vivo* model of neuroinflammation has been shown to produce large lesions
434 accompanied by an inflammatory response involving increased microglial activation and an
435 axon-sparing neurodegeneration which is directly associated with the degree of brain
436 damage [52,53]. This leads to an increase in the expression of TSPO [39,40,46]. This
437 mitochondrial protein is considered to be a sensitive biomarker of microglial activation [54]
438 and specific imaging tracers are currently used to explore it in preclinical and clinical studies
439 [55-58]. We evaluated this molecular target by quantitative autoradiography. [³H]PK-11195 is
440 a long used tracer in this type of experiment, and the tritiated homolog of the new generation
441 tracer of TSPO, DPA-714, has been recently developed [41]. First, we compared the
442 properties of both of these tracers in our QA rat model and demonstrated that [³H]DPA-714
443 displayed a lower non specific binding than [³H]PK-11195. This result is in agreement with *in*
444 *vivo* experiments which observed a higher signal-to-noise ratio using [¹⁸F]DPA-714 in
445 comparison to [¹¹C]PK-11195 in different rodent models such as in middle cerebral artery
446 occlusion (MCAO) [59] and herpes encephalitis (HSE) [60]. In addition, higher inter-animal
447 variability in MCAO and HSE models was observed than in our QA model. Thus, we used the

448 tritiated analog of a highly sensitive marker of TSPO that can also be used for *in vivo* human
449 clinical investigations. Then, we examined whether the PHA 543613 effects on TSPO binding
450 with [³H]DPA-714 were dose-related in our model; the compound was administered at the
451 concentrations of 6 mg/kg [28] or 12 mg/kg. The TSPO bindings levels illustrated significant
452 decrease of inflammation in QA-PHA12 vs sham animals while the rate of increase of TSPO
453 binding in IL vs CL striatum did not decrease significantly between QA-PHA6 and sham
454 group. As a result of this finding and since no difference in body weight or animal
455 compartment were noticed between control, QA-PHA6 and QA-PHA12 animals, we decided
456 to make further experiments with the highest dose of PHA 543613.

457

458 Effects associated to $\alpha 7$ nAChRs agonist depend on various parameters like the levels of
459 $\alpha 7$ nAChRs expression and function or the neuropathology stage and intrinsic properties of
460 the $\alpha 7$ nAChR agonists [61]. $\alpha 7$ nAChRs are known to be widely expressed throughout
461 several brain regions in mammals by neurons and glial cells. Among them, the $\alpha 7$ nAChRs
462 are probably the most widespread nAChRs subtype expressed in the brain [62]. These
463 receptors can control the release of various types of neurotransmitters, contribute to synaptic
464 plasticity and they have been proved to participate in the regulation of inflammatory reactions
465 [63]. However, the rapid desensitization of $\alpha 7$ nAChRs is considered an important factor
466 limiting its potential therapeutic use. Therefore, to approach the mechanism that could
467 explain the beneficial effect of PHA 543613 on neuroinflammation, we quantified $\alpha 7$ nAChRs
468 expression in both IL and CL striata of Sham, PHA 6mg/kg and PHA 12mg/kg QA-lesioned
469 animals. Autoradiography binding with alpha-bungarotoxin was performed at 4-days post-
470 lesion and confirmed the expression of $\alpha 7$ nAChRs in the striatum of all groups of rats. In
471 addition, we observed a decreasing of binding in IL vs CL striatum in Sham, PHA6 and
472 PHA12 rats, hypothetically reflecting the tissue destruction and thus neuron and glial cell loss
473 induced in all animals by local QA injection. This result could also be consistent with a recent
474 publication reporting that neuroinflammation induced by regular bacterial lipopolysaccharide
475 injections resulted in the decrease of $\alpha 7$ nAChRs density in the brain of mice [64]. Indeed,

476 after activation, the $\alpha 7$ nAChRs undergo rapid desensitivation in order to limit the influx of
477 calcium (Ca^{2+}) into the cell which could lead to a phenomenon of excitotoxicity [65]. However,
478 4-day chronic treatment with PHA 543613 did not lead to a significant modification of
479 $\alpha 7$ nAChRs expression vs control which reveals no significant receptor desensitivation. This
480 observation probably does not apply to our short-term PHA exposure suggesting no induced
481 receptor desensitivation. Lastly, it is then noteworthy that in spite of the diminution of
482 $\alpha 7$ nAChRs expression in lesioned striatum of PHA12-treated animals, neuroprotective and
483 anti-inflammatory effects of the drug were observed.

484

485 The effects of the PHA 543613 treatment on microglial activation in striatum were also
486 assessed by immunohistochemistry using Ox-42 - an antibody specific to CD11b mostly
487 expressed in activated microglia. Measurements showed in both QA-PHA12 and Sham
488 groups a significant massive increase of Cd11b expression in the striatum from the IL
489 hemisphere vs CL hemisphere, confirming the inflammatory impact of QA injection on
490 microglial cell activity. Interestingly, the number of cells expressing the CD11b was
491 significantly (-25.5%) lower in IL striatum of QA-PHA12 rats than in IL striatum of Sham rats.
492 To evaluate the potential effect of PHA543613 treatment on neuron survival in striatum, we
493 used Neun marker located in the nucleus and the perinuclear cytoplasm of postmitotic
494 neurons in mammals. We logically observed significant reduction in neuron population in IL
495 striatum vs CL of both QA-PHA12 and Sham groups, illustrating once again the deleterious
496 effect of QA injected locally. However, considering IL striatum counting of both QA-PHA12
497 and Sham rats, it is noteworthy that the number of preserved neurons was approximately
498 twice as high in the QA-PHA12 than in the Sham group, illustrating the protective effect
499 mediated by PHA treatment in IL striatum of treated animals. Those results indicate that the
500 neuroprotective effects on the striatal neurons are associated with a reduction in microglial
501 activation. Although QA exerts the greatest damage to neurons where NMDA receptors are
502 present, cholinergic and GABAergic neuronal cell types seem to be more sensitive than
503 others especially in the striatum [49,66]. Thus, these two types of neurons do not seem to be

504 involved in the beneficial effects observed following administration of PHA 543613 in our
505 study.

506

507 We report here through the first evaluation of the $\alpha 7$ nAChRs agonist PHA 543613 in an *in*
508 *vivo* excitotoxic model of neuroinflammation, the strong relationship that exists between the
509 effects of PHA 543613 on neuroinflammation and neuron integrity. We confirm that PHA
510 543613 can reduce both neuronal loss and microglial activation in the same animals, as
511 already observed in a rat model of Parkinson's disease [28]. The $\alpha 7$ nAChRs are able to
512 mediate the anti-inflammatory effect of acetylcholine by attenuating the pro-inflammatory
513 cytokine release involved in the regulation of the cholinergic anti-inflammatory pathway in
514 brain astrocytes or microglia [67]. However, $\alpha 7$ nAChRs chronic stimulation has been
515 associated with massive and persistent calcium increase inside brain cells well known to be
516 toxic to cells expressing this receptor [68]. This statement supports the necessity to pay
517 attention to the duration of $\alpha 7$ nAChRs agonist regimen when used for a therapeutic purpose.
518 Indeed, we have demonstrated the capability of a $\alpha 7$ nAChRs-activating agent to induce fast
519 neuroprotection facing an acute brain traumatic injury; these findings support the short-term
520 use of $\alpha 7$ nAChRs-activating agents as a strategy to reduce traumatic brain injury triggered
521 BBB permeability [69]. Considering that PHA 543613 can target both of the processes
522 involved in most neurodegenerative diseases, $\alpha 7$ nAChRs agonists could represent a major
523 therapeutic challenge in neurology.

524

525

526

527

528

529

530

531

532 **List of abbreviations**

533 AD: Alzheimer disease

534 BBB: blood brain barrier

535 CL: contra lateral

536 cpm: counts per min

537 HSE: herpes encephalitis

538 IL: ipsi lateral

539 i.p: intraperitoneal

540 α 7nAChRs: nicotinic acetylcholine receptor α 7

541 MCAO: middle cerebral artery occlusion

542 NeuN: neuronal nuclei

543 NMDA: N-methyl-D-aspartate

544 NO: nitric oxyde

545 PD: Parkinson disease

546 QA: quinolinic acid

547 ROIs: regions of interest

548 RT: room temperature

549 SEM: standard error of the mean

550 TSPO: 18kDa translocator protein

551 Vs: versus

552

553

554

555

556

557

558

559

560 **Ethics approval**

561 All procedures were conducted in accordance with the European Community Council
562 Directive 2010/63/EU for laboratory animal care and the experimental protocol was validated
563 by the Regional Ethical Committee (Authorization N°2015022011523044).

564

565 **Competing interest**

566 The authors declare that they have no competing interests.

567

568 **Authors' contributions**

569 SC and DA contributed equally to this work.

570

571 **Availability of data and materials**

572 The datasets during and/or analysed during the current study available from the
573 corresponding author on reasonable request.

574

575 **Acknowledgements**

576 This work was supported by the Région Centre-Val de Loire (2014 00094049 - AP 2014-
577 850) and the European Union's Seventh Framework Programme (FP7/2007-2013) under
578 grant agreement n°278850 (INMiND). Authors thank Sylvie Bodard and Zuhail Gulhan for
579 technical assistance.

580

581 **Consent for publication**

582 Not applicable

583

584 **Funding**

585 Not applicable

586

587

588 **References**

- 589 1. Takahashi K, Funata N, Ikuta F, Sato S. Neuronal apoptosis and inflammatory
590 responses in the central nervous system of a rabbit treated with Shiga toxin-2. *J*
591 *Neuroinflammation*. 2008;5:11.
- 592 2. Block ML, Hong J-S. Microglia and inflammation-mediated neurodegeneration: multiple
593 triggers with a common mechanism. *Prog Neurobiol*. 2005 Jun;76(2):77–98.
- 594 3. Smith JA, Das A, Ray SK, Banik NL. Role of pro-inflammatory cytokines released from
595 microglia in neurodegenerative diseases. *Brain Res Bull*. 2012 Jan 4;87(1):10–20.
- 596 4. Haynes SE, Hollopeter G, Yang G, Kurpius D, Dailey ME, Gan W-B, et al. The P2Y12
597 receptor regulates microglial activation by extracellular nucleotides. *Nat Neurosci*. 2006
598 Dec;9(12):1512–9.
- 599 5. Hoozemans JJM, Veerhuis R, Rozemuller AJM, Arendt T, Eikelenboom P. Neuronal
600 COX-2 expression and phosphorylation of pRb precede p38 MAPK activation and
601 neurofibrillary changes in AD temporal cortex. *Neurobiol Dis*. 2004 Apr;15(3):492–9.
- 602 6. Glass CK, Saijo K, Winner B, Marchetto MC, Gage FH. Mechanisms Underlying
603 Inflammation in Neurodegeneration. *Cell*. 2010 Mar 19;140(6):918–34.
- 604 7. Bartels AL, Willemsen ATM, Doorduyn J, de Vries EFJ, Dierckx RA, Leenders KL. [11C]-
605 PK11195 PET: quantification of neuroinflammation and a monitor of anti-inflammatory
606 treatment in Parkinson's disease? *Parkinsonism Relat Disord*. 2010 Jan;16(1):57–9.
- 607 8. Gordon PH, Moore DH, Miller RG, Florence JM, Verheijde JL, Doorish C, et al. Efficacy
608 of minocycline in patients with amyotrophic lateral sclerosis: a phase III randomised
609 trial. *Lancet Neurol*. 2007 Dec;6(12):1045–53.
- 610 9. Huntington Study Group DOMINO Investigators. A futility study of minocycline in
611 Huntington's disease. *Mov Disord Off J Mov Disord Soc*. 2010 Oct 15;25(13):2219–24.

- 612 10. Relkin N. Clinical trials of intravenous immunoglobulin for Alzheimer's disease. *J Clin*
613 *Immunol.* 2014 Jul;34 Suppl 1:S74-79.
- 614 11. Zhang Y, Metz LM, Yong VW, Bell RB, Yeung M, Patry DG, et al. Pilot study of
615 minocycline in relapsing-remitting multiple sclerosis. *Can J Neurol Sci J Can Sci Neurol.*
616 2008 May;35(2):185-91.
- 617 12. Gotti C, Clementi F. Neuronal nicotinic receptors: from structure to pathology. *Prog*
618 *Neurobiol.* 2004 Dec;74(6):363-96.
- 619 13. O'Reilly EJ, McCullough ML, Chao A, Jane Henley S, Calle EE, Thun MJ, et al.
620 Smokeless tobacco use and the risk of Parkinson's disease mortality. *Mov Disord.* 2005
621 Oct 1;20(10):1383-4.
- 622 14. Searles Nielsen S, Gallagher LG, Lundin JI, Longstreth W t., Smith-Weller T, Franklin
623 GM, et al. Environmental tobacco smoke and Parkinson's disease. *Mov Disord.* 2012
624 Feb 1;27(2):293-7.
- 625 15. Thacker EL, O'Reilly EJ, Weisskopf MG, Chen H, Schwarzschild MA, McCullough ML,
626 et al. Temporal relationship between cigarette smoking and risk of Parkinson disease.
627 *Neurology.* 2007 Jun 3;68(10):764-8.
- 628 16. Newhouse P, Kellar K, Aisen P, White H, Wesnes K, Coderre E, et al. Nicotine
629 treatment of mild cognitive impairment: a 6-month double-blind pilot clinical trial.
630 *Neurology.* 2012 Jan 10;78(2):91-101.
- 631 17. Villafane G, Cesaro P, Rialland A, Baloul S, Azimi S, Bourdet C, et al. Chronic high
632 dose transdermal nicotine in Parkinson's disease: an open trial. *Eur J Neurol.* 2007 Dec
633 1;14(12):1313-6.

- 634 18. Itti E, Villafane G, Malek Z, Brugières P, Capacchione D, Itti L, et al. Dopamine
635 transporter imaging under high-dose transdermal nicotine therapy in Parkinson's
636 disease: an observational study. *Nucl Med Commun*. 2009 Jul;30(7):513–8.
- 637 19. Holmes AD, Copland DA, Silburn PA, Chenery HJ. Acute nicotine enhances strategy-
638 based semantic processing in Parkinson's disease. *Int J Neuropsychopharmacol Off*
639 *Sci J Coll Int Neuropsychopharmacol CINP*. 2011 Aug;14(7):877–85.
- 640 20. Vieregge A, Sieberer M, Jacobs H, Hagenah JM, Vieregge P. Transdermal nicotine in
641 PD A randomized, double-blind, placebo-controlled study. *Neurology*. 2001 Sep
642 25;57(6):1032–5.
- 643 21. Dineley KT, Pandya AA, Yakel JL. Nicotinic ACh receptors as therapeutic targets in
644 CNS disorders. *Trends Pharmacol Sci*. 2015 Feb;36(2):96–108.
- 645 22. Gahring LC, Persiyarov K, Dunn D, Weiss R, Meyer EL, Rogers SW. Mouse strain-
646 specific nicotinic acetylcholine receptor expression by inhibitory interneurons and
647 astrocytes in the dorsal hippocampus. *J Comp Neurol*. 2004 Jan 12;468(3):334–46.
- 648 23. Jensen AA, Frølund B, Liljefors T, Krogsgaard-Larsen P. Neuronal nicotinic
649 acetylcholine receptors: structural revelations, target identifications, and therapeutic
650 inspirations. *J Med Chem*. 2005 Jul 28;48(15):4705–45.
- 651 24. Prickaerts J, van Goethem NP, Chesworth R, Shapiro G, Boess FG, Methfessel C, et
652 al. EVP-6124, a novel and selective $\alpha 7$ nicotinic acetylcholine receptor partial agonist,
653 improves memory performance by potentiating the acetylcholine response of $\alpha 7$
654 nicotinic acetylcholine receptors. *Neuropharmacology*. 2012 Feb;62(2):1099–110.
- 655 25. Quik M, Zhang D, McGregor M, Bordia T. Alpha7 nicotinic receptors as therapeutic
656 targets for Parkinson's disease. *Biochem Pharmacol*. 2015 Oct 15;97(4):399–407.

- 657 26. Bordia T, McGregor M, Papke RL, Decker MW, Michael McIntosh J, Quik M. The $\alpha 7$
658 nicotinic receptor agonist ABT-107 protects against nigrostriatal damage in rats with
659 unilateral 6-hydroxydopamine lesions. *Exp Neurol*. 2015 Jan;263:277–84.
- 660 27. Di Paolo T, Grégoire L, Feuerbach D, Elbast W, Weiss M, Gomez-Mancilla B. AQW051,
661 a novel and selective nicotinic acetylcholine receptor $\alpha 7$ partial agonist, reduces l-Dopa-
662 induced dyskinesias and extends the duration of l-Dopa effects in parkinsonian
663 monkeys. *Parkinsonism Relat Disord*. 2014 Nov;20(11):1119–23.
- 664 28. Sérrière S, Doméné A, Vercouillie J, Mothes C, Bodard S, Rodrigues N, et al.
665 Assessment of the Protection of Dopaminergic Neurons by an $\alpha 7$ Nicotinic Receptor
666 Agonist, PHA 543613 Using [(18)F]LBT-999 in a Parkinson's Disease Rat Model. *Front*
667 *Med*. 2015;2:61.
- 668 29. Krafft PR, Altay O, Rolland WB, Duris K, Lekic T, Tang J, et al. $\alpha 7$ Nicotinic
669 Acetylcholine Receptor Agonism Confers Neuroprotection Through GSK-3 β Inhibition in
670 a Mouse Model of Intracerebral Hemorrhage. *Stroke*. 2012 Jan 3;43(3):844–50.
- 671 30. Krafft PR, Caner B, Klebe D, Rolland WB, Tang J, Zhang JH. PHA-543613 preserves
672 blood-brain barrier integrity after intracerebral hemorrhage in mice. *Stroke J Cereb Circ*.
673 2013 Jun;44(6):1743–7.
- 674 31. Barrio L del, Martín-de-Saavedra MD, Romero A, Parada E, Egea J, Avila J, et al.
675 Neurotoxicity Induced by Okadaic Acid in the Human Neuroblastoma SH-SY5Y Line
676 Can Be Differentially Prevented by $\alpha 7$ and $\beta 2^*$ Nicotinic Stimulation. *Toxicol Sci*. 2011
677 Jan 9;123(1):193–205.
- 678 32. Rosas-Ballina M, Ochani M, Parrish WR, Ochani K, Harris YT, Huston JM, et al. Splenic
679 nerve is required for cholinergic antiinflammatory pathway control of TNF in
680 endotoxemia. *Proc Natl Acad Sci U S A*. 2008 Aug 5;105(31):11008–13.

- 681 33. Wishka DG, Walker DP, Yates KM, Reitz SC, Jia S, Myers JK, et al. Discovery of N-
682 [(3R)-1-azabicyclo[2.2.2]oct-3-yl]furo[2,3-c]pyridine-5-carboxamide, an agonist of the
683 alpha7 nicotinic acetylcholine receptor, for the potential treatment of cognitive deficits in
684 schizophrenia: synthesis and structure--activity relationship. *J Med Chem.* 2006 Jul
685 13;49(14):4425–36.
- 686 34. Acker BA, Jacobsen EJ, Rogers BN, Wishka DG, Reitz SC, Piotrowski DW, et al.
687 Discovery of N-[(3R,5R)-1-azabicyclo[3.2.1]oct-3-yl]furo[2,3-c]pyridine-5-carboxamide
688 as an agonist of the alpha7 nicotinic acetylcholine receptor: in vitro and in vivo activity.
689 *Bioorg Med Chem Lett.* 2008 Jun 15;18(12):3611–5.
- 690 35. Sadigh-Eteghad S, Mahmoudi J, Babri S, Talebi M, Sadigh-Eteghad S, Mahmoudi J, et
691 al. Effect of alpha-7 nicotinic acetylcholine receptor activation on beta-amyloid induced
692 recognition memory impairment. Possible role of neurovascular function. *Acta Cir Bras.*
693 2015 Nov;30(11):736–42.
- 694 36. Ransohoff RM. How neuroinflammation contributes to neurodegeneration. *Science.*
695 2016 Aug 19;353(6301):777–83.
- 696 37. Estrada Sánchez AM, Mejía-Toiber J, Massieu L. Excitotoxic neuronal death and the
697 pathogenesis of Huntington's disease. *Arch Med Res.* 2008 Apr;39(3):265–76.
- 698 38. Schwarcz R, Köhler C. Differential vulnerability of central neurons of the rat to quinolinic
699 acid. *Neurosci Lett.* 1983 Jul 15;38(1):85–90.
- 700 39. Arlicot N, Katsifis A, Garreau L, Mattner F, Vergote J, Duval S, et al. Evaluation of
701 CLINDE as potent translocator protein (18 kDa) SPECT radiotracer reflecting the
702 degree of neuroinflammation in a rat model of microglial activation. *Eur J Nucl Med Mol*
703 *Imaging.* 2008 Dec;35(12):2203–11.

- 704 40. Arlicot N, Tronel C, Bodard S, Garreau L, de la Crompe B, Vandeveld I, et al.
705 Translocator protein (18 kDa) mapping with [125I]-CLINDE in the quinolinic acid rat
706 model of excitotoxicity: a longitudinal comparison with microglial activation, astrogliosis,
707 and neuronal death. *Mol Imaging*. 2014;13:4–11.
- 708 41. Damont A, Garcia-Argote S, Buisson D-A, Rousseau B, Dollé F. Efficient tritiation of the
709 translocator protein (18 kDa) selective ligand DPA-714. *J Label Compd Radiopharm*.
710 2015 Jan;58(1):1–6.
- 711 42. Dr GP, Watson C. *The Rat Brain in Stereotaxic Coordinates: Compact*. 6th ed.
712 Academic Press; 2008.
- 713 43. Shytle RD, Mori T, Townsend K, Vendrame M, Sun N, Zeng J, et al. Cholinergic
714 modulation of microglial activation by alpha 7 nicotinic receptors. *J Neurochem*. 2004
715 Apr;89(2):337–43.
- 716 44. Kalkman HO, Feuerbach D. Modulatory effects of $\alpha 7$ nAChRs on the immune system
717 and its relevance for CNS disorders. *Cell Mol Life Sci CMLS*. 2016 Jul;73(13):2511–30.
- 718 45. de Jonge WJ, Ulloa L. The alpha7 nicotinic acetylcholine receptor as a pharmacological
719 target for inflammation. *Br J Pharmacol*. 2007 Aug;151(7):915–29.
- 720 46. Moresco RM, Lavazza T, Belloli S, Lecchi M, Pezzola A, Todde S, et al. Quinolinic acid
721 induced neurodegeneration in the striatum: a combined in vivo and in vitro analysis of
722 receptor changes and microglia activation. *Eur J Nucl Med Mol Imaging*. 2008
723 Apr;35(4):704–15.
- 724 47. Alexi T, Borlongan CV, Faull RL, Williams CE, Clark RG, Gluckman PD, et al.
725 Neuroprotective strategies for basal ganglia degeneration: Parkinson's and
726 Huntington's diseases. *Prog Neurobiol*. 2000 Apr;60(5):409–70.

- 727 48. Beal MF, Kowall NW, Ellison DW, Mazurek MF, Swartz KJ, Martin JB. Replication of the
728 neurochemical characteristics of Huntington's disease by quinolinic acid. *Nature*. 1986
729 May 8;321(6066):168–71.
- 730 49. Pérez-De La Cruz V, Königsberg M, Santamaría A. Kynurenine pathway and disease:
731 an overview. *CNS Neurol Disord Drug Targets*. 2007 Dec;6(6):398–410.
- 732 50. Guillemin GJ. Quinolinic acid, the inescapable neurotoxin. *FEBS J*. 2012
733 Apr;279(8):1356–65.
- 734 51. Nicholls DG. Mitochondrial dysfunction and glutamate excitotoxicity studied in primary
735 neuronal cultures. *Curr Mol Med*. 2004 Mar;4(2):149–77.
- 736 52. Kreutzberg GW. Microglia: a sensor for pathological events in the CNS. *Trends*
737 *Neurosci*. 1996 Aug;19(8):312–8.
- 738 53. Heneka MT, Rodríguez JJ, Verkhratsky A. Neuroglia in neurodegeneration. *Brain Res*
739 *Rev*. 2010 May;63(1–2):189–211.
- 740 54. Chen M-K, Guilarte TR. Translocator protein 18 kDa (TSPO): molecular sensor of brain
741 injury and repair. *Pharmacol Ther*. 2008 Apr;118(1):1–17.
- 742 55. Venneti S, Lopresti BJ, Wiley CA. The peripheral benzodiazepine receptor
743 (Translocator protein 18kDa) in microglia: from pathology to imaging. *Prog Neurobiol*.
744 2006 Dec;80(6):308–22.
- 745 56. Chauveau F, Van Camp N, Dollé F, Kuhnast B, Hinnen F, Damont A, et al. Comparative
746 evaluation of the translocator protein radioligands 11C-DPA-713, 18F-DPA-714, and
747 11C-PK11195 in a rat model of acute neuroinflammation. *J Nucl Med Off Publ Soc Nucl*
748 *Med*. 2009 Mar;50(3):468–76.

- 749 57. Corcia P, Tauber C, Vercoullie J, Arlicot N, Prunier C, Praline J, et al. Molecular
750 imaging of microglial activation in amyotrophic lateral sclerosis. *PloS One*.
751 2012;7(12):e52941.
- 752 58. Hamelin L, Lagarde J, Dorothée G, Leroy C, Labit M, Comley RA, et al. Early and
753 protective microglial activation in Alzheimer's disease: a prospective study using 18F-
754 DPA-714 PET imaging. *Brain J Neurol*. 2016 Apr;139(Pt 4):1252–64.
- 755 59. Boutin H, Prenant C, Maroy R, Galea J, Greenhalgh AD, Smigova A, et al. [18F]DPA-
756 714: direct comparison with [11C]PK11195 in a model of cerebral ischemia in rats. *PloS*
757 *One*. 2013;8(2):e56441.
- 758 60. Doorduyn J, Klein HC, Dierckx RA, James M, Kassiou M, de Vries EFJ. [11C]-DPA-713
759 and [18F]-DPA-714 as new PET tracers for TSPO: a comparison with [11C]-(R)-
760 PK11195 in a rat model of herpes encephalitis. *Mol Imaging Biol MIB Off Publ Acad Mol*
761 *Imaging*. 2009 Dec;11(6):386–98.
- 762 61. Shen J, Wu J. Nicotinic Cholinergic Mechanisms in Alzheimer's Disease. *Int Rev*
763 *Neurobiol*. 2015;124:275–92.
- 764 62. Zoli M, Pistillo F, Gotti C. Diversity of native nicotinic receptor subtypes in mammalian
765 brain. *Neuropharmacology*. 2015 Sep;96(Pt B):302–11.
- 766 63. Soria-Fregozo C, Flores-Soto ME, Pérez-Vega MI, Feria-Velasco A. 5-HT denervation
767 of the adult rat prefrontal cortex induces changes in the expression of $\alpha 4$ and $\alpha 7$
768 nicotinic acetylcholine receptor subtypes. *Neurol Barc Spain*. 2013 May;28(4):212–8.
- 769 64. Lykhmus O, Gergalova G, Zouridakis M, Tzartos S, Komisarenko S, Skok M.
770 Inflammation decreases the level of alpha7 nicotinic acetylcholine receptors in the brain
771 mitochondria and makes them more susceptible to apoptosis induction. *Int*
772 *Immunopharmacol*. 2015 Nov;29(1):148–51.

- 773 65. Zhang Z, Vijayaraghavan S, Berg DK. Neuronal acetylcholine receptors that bind α -
774 bungarotoxin with high affinity function as ligand-gated ion channels. *Neuron*. 1994 Jan
775 1;12(1):167–77.
- 776 66. Lugo-Huitrón R, Ugalde Muñiz P, Pineda B, Pedraza-Chaverrí J, Ríos C, Pérez-de la
777 Cruz V. Quinolinic acid: an endogenous neurotoxin with multiple targets. *Oxid Med Cell*
778 *Longev*. 2013;2013:104024.
- 779 67. Stuckenholz V, Bacher M, Balzer-Geldsetzer M, Alvarez-Fischer D, Oertel WH, Dodel
780 RC, et al. The $\alpha 7$ nAChR agonist PNU-282987 reduces inflammation and MPTP-
781 induced nigral dopaminergic cell loss in mice. *J Park Dis*. 2013;3(2):161–72.
- 782 68. Williams DK, Peng C, Kimbrell MR, Papke RL. Intrinsically low open probability of $\alpha 7$
783 nicotinic acetylcholine receptors can be overcome by positive allosteric modulation and
784 serum factors leading to the generation of excitotoxic currents at physiological
785 temperatures. *Mol Pharmacol*. 2012 Oct;82(4):746–59.
- 786 69. Dash PK, Zhao J, Kobori N, Redell JB, Hylín MJ, Hood KN, et al. Activation of Alpha 7
787 Cholinergic Nicotinic Receptors Reduce Blood-Brain Barrier Permeability following
788 Experimental Traumatic Brain Injury. *J Neurosci Off J Soc Neurosci*. 2016 Mar
789 2;36(9):2809–18.

790

791 **Figure legends**

792 **Figure 1: Comparative evaluation of TSPO radioligands [³H]DPA-714 and [³H]PK-11195**

793 **by autoradiographic study. (A)** Representative autoradiographic images obtained on 16

794 μm-thick coronal brain sections with [³H]PK-11195 (1 nmol/L, left panel) and [³H]DPA-714 (1

795 nmol/L, right panel) alone or in presence of stable PK11195 (1 μmol/L, in the right of each

796 panel) of the same animal. **(B)** Percentage of TSPO specific binding in IL vs CL striatum

797 (mean % ± SEM) from QA lesioned rats (n= 9) with [³H]PK-11195 or [³H]DPA-714. **(C)**

798 Correlation between [³H]PK-11195 and [³H]DPA-714 autoradiography study. The correlation

799 is reported for the percentage of TSPO binding in IL vs CL striatum with each tracer. #p<0.05

800 (Mann Whitney test). *p<0.05 (two-tailed Spearman test). Abbreviations: CL:

801 contralateral; IL: ipsilateral; SEM: standard error of the mean.

802

803 **Figure 2: Autoradiographic analysis of TSPO density with [³H]DPA-714 in the striatum.**

804 **(A)** Representative total (left side) and non-specific (right side) binding of [³H]DPA-714

805 obtained on 16 μm-thick coronal brain section in Sham rats (upper panel), QA-PHA 6 and

806 QA-PHA12 rats (lower panel). **(B)** Percentage increase of TSPO binding in IL vs CL striatum

807 (mean % ± SEM) from Sham (n= 5), QA-PHA6 (n= 8) and QA-PHA12 (n= 9) rats.

808 Abbreviations: CL: contralateral; IL: ipsilateral; SEM: standard error of the mean.

809

810 **Figure 3: Autoradiographic analysis of α7nAChRs density with [¹²⁵I]α-bungarotoxin in**

811 **the striatum. (A)** Representative total (left side) and non-specific (right side) binding of

812 [¹²⁵I]α-bungarotoxin obtained on 16 μm-thick coronal brain section in Sham rats (upper

813 panel), QA-PHA 6 and QA-PHA12 rats (lower panel). **(B)** α7nAChRs expression in IL and CL

814 striatum from Sham (n=6), QA-PHA6 (n=6) and QA-PHA12 (n=6) rats. Data are expressed

815 as cpm/mm². Abbreviations : CL: contralateral; IL: ipsilateral; cpm/mm²: counts per min per

816 mm².

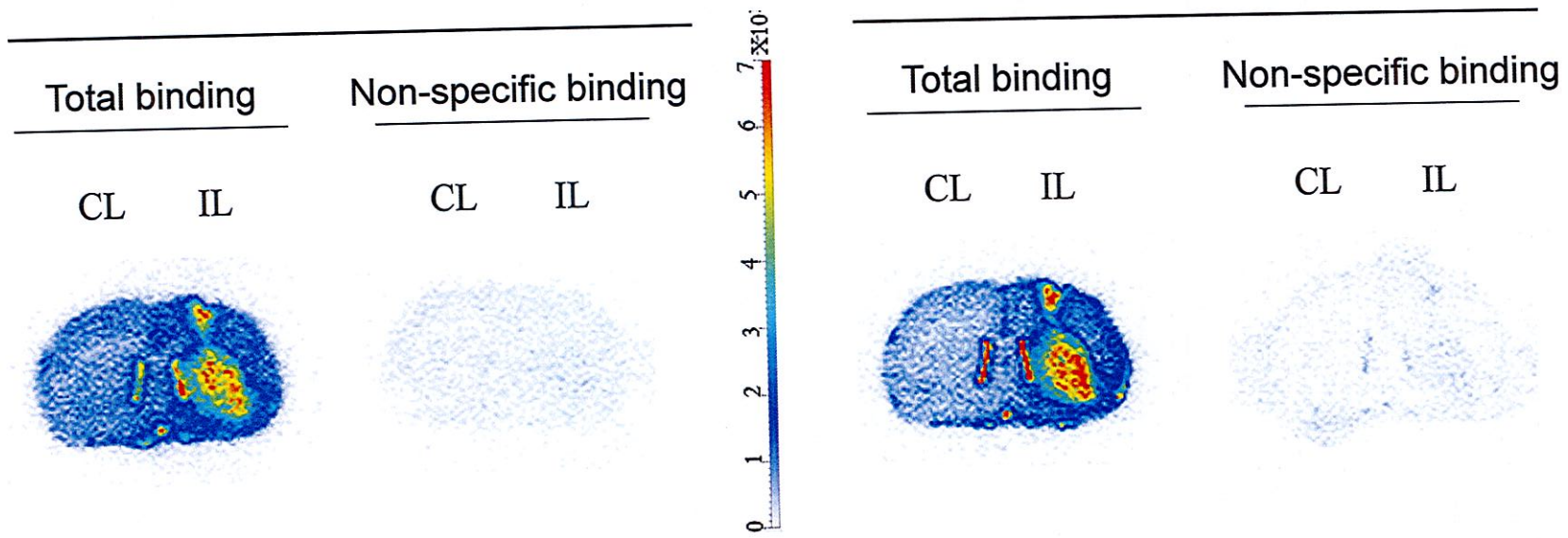
817

818 **Figure 4: Immunofluorescence in rat striatum of Ox-42 in Sham group and QA-PHA12**
819 **group. (A)** Coronal rat brain representation. The full line and areas marked in red symbolize,
820 respectively, the site of injury and areas where Ox-42 immunofluorescence was performed.
821 **(B)** Representative immunofluorescence images of activated microglia by Ox-42 staining
822 (green channel) and DAPI (blue channel) in the CL (left) and IL (right) striatum of Sham
823 (upper) (n=6) and QA-PHA12 (lower) (n=6) rats. Magnification was x 20. Scale bar, 50 μ m.
824 **(C)** Ox-42 expression in IL and CL striatum for each group. Data are expressed as number of
825 cells expressing Ox-42 marker. **(D)** Data are expressed as relative activated microglia in IL
826 vs CL striatum for each group. # $p < 0.05$ (Mann Whitney test). * $p < 0.05$ (Wilcoxon test).
827 Abbreviations: CL: contralateral; IL: ipsilateral.

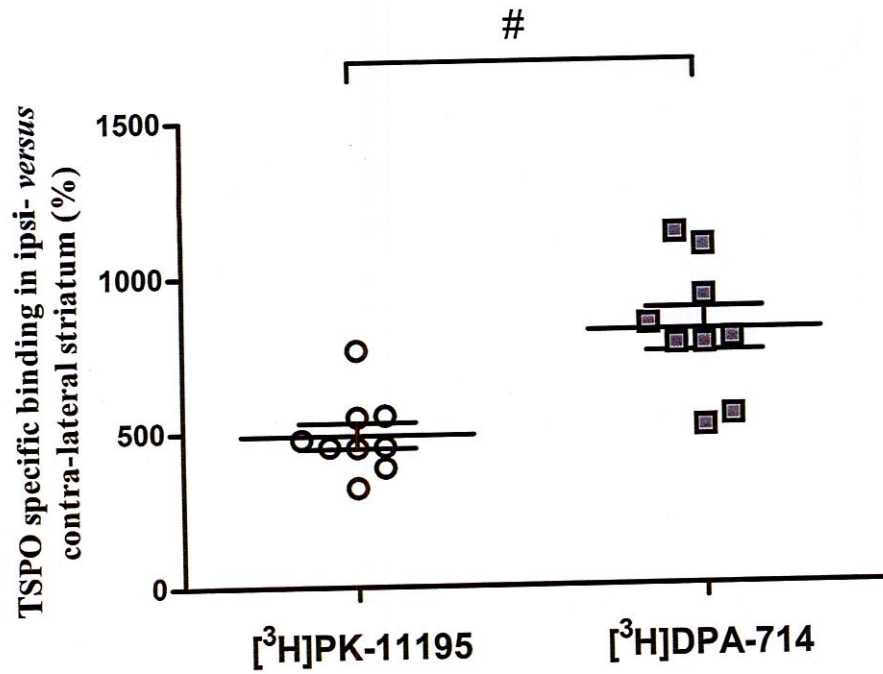
828

829 **Figure 5: Immunofluorescence in rat striatum of neurons (NeuN) in Sham group and**
830 **QA-PHA12 group. (A)** Coronal rat brain representation. The full line and areas marked in
831 red symbolize, respectively, the site of injury and areas where NeuN immunofluorescence
832 was performed. **(B)** Representative immunofluorescence images of neurons by NeuN
833 staining (green channel) and DAPI (blue channel) in the CL (left) and IL (right) striatum of
834 Sham (upper) (n=6) and QA-PHA12 (lower) (n=6) rats. **(C)** Neuronal expression in CL and IL
835 striatum for each group. Data are expressed as number of cells expressing NeuN marker.
836 **(D)** Data are expressed as relative neuronal loss in IL vs CL striatum for each group #
837 $p < 0.05$ (Mann Whitney test). * $p < 0.05$ (Wilcoxon test). Abbreviations: CL: contralateral; IL:
838 ipsilateral.

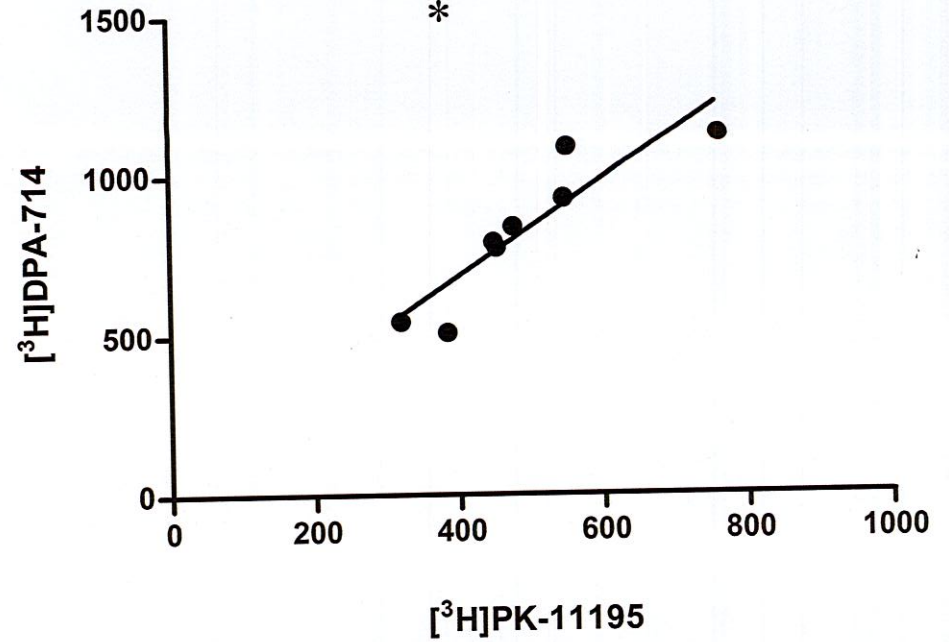
839

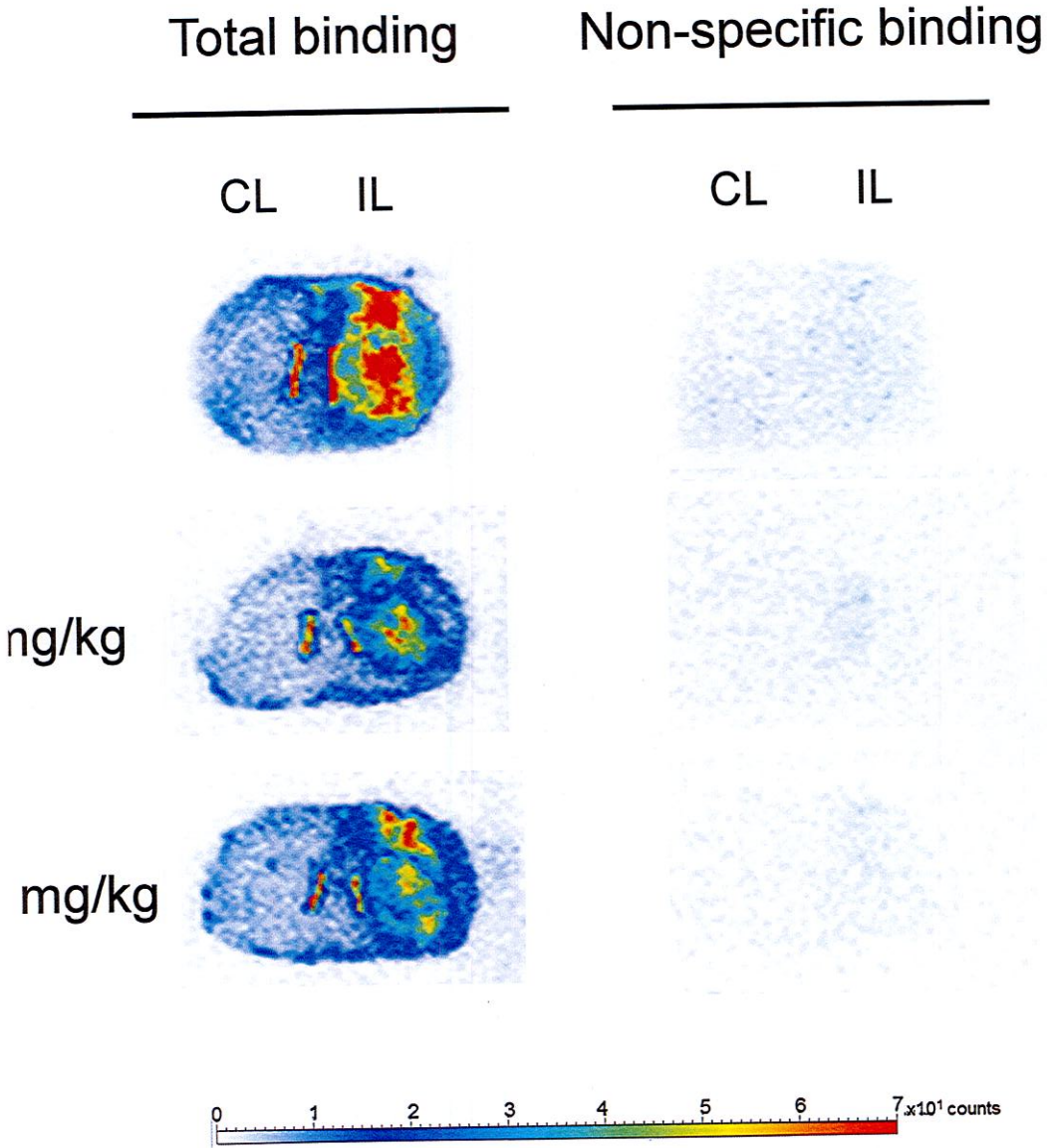


B

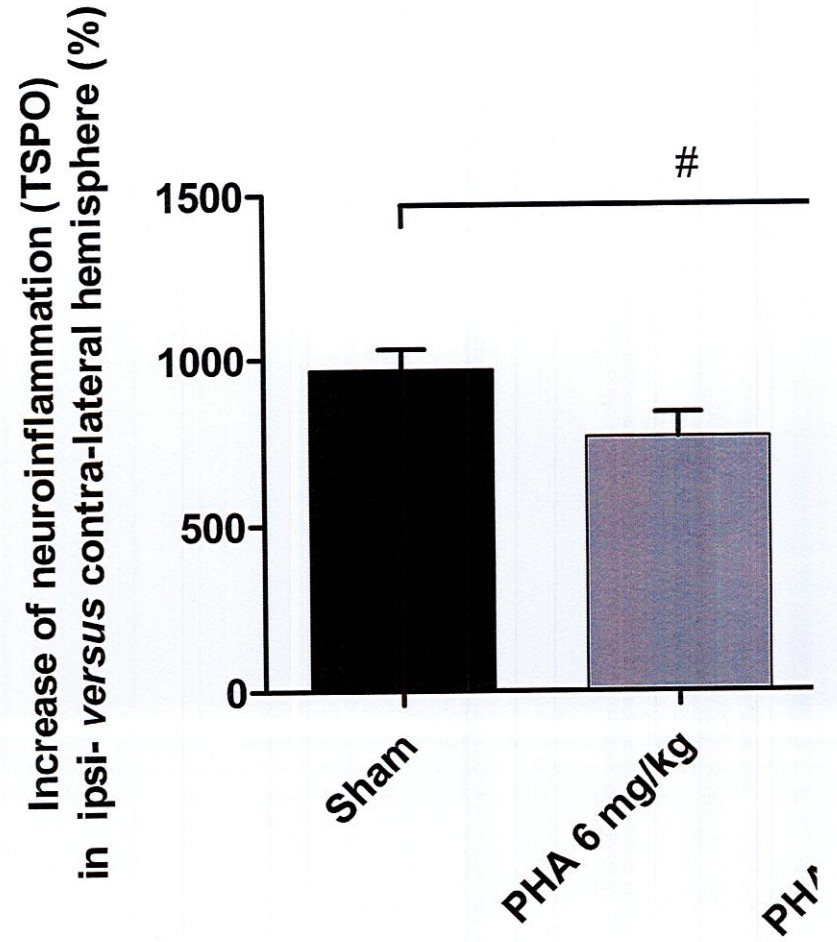


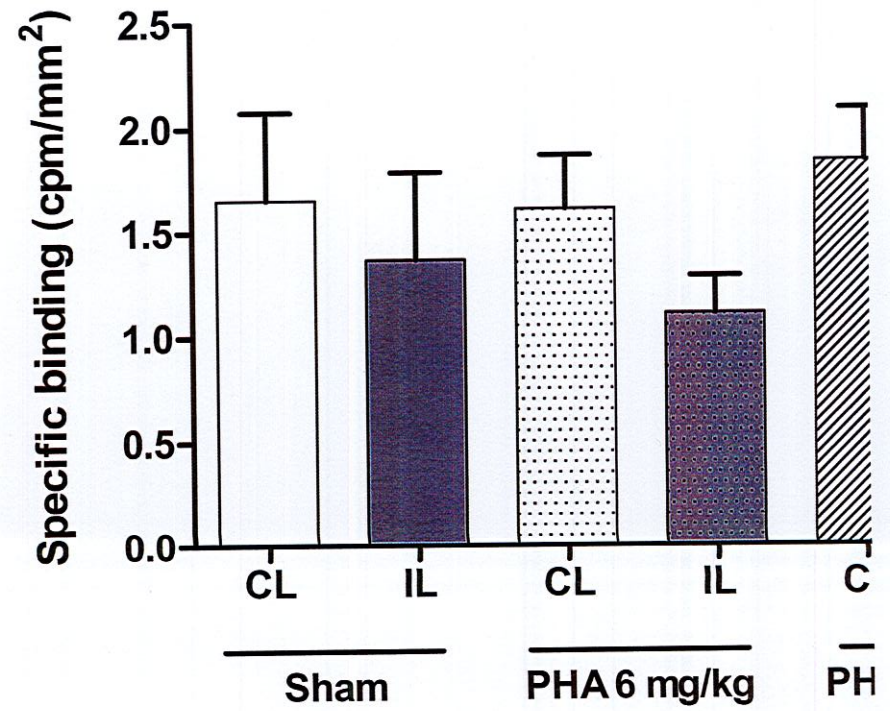
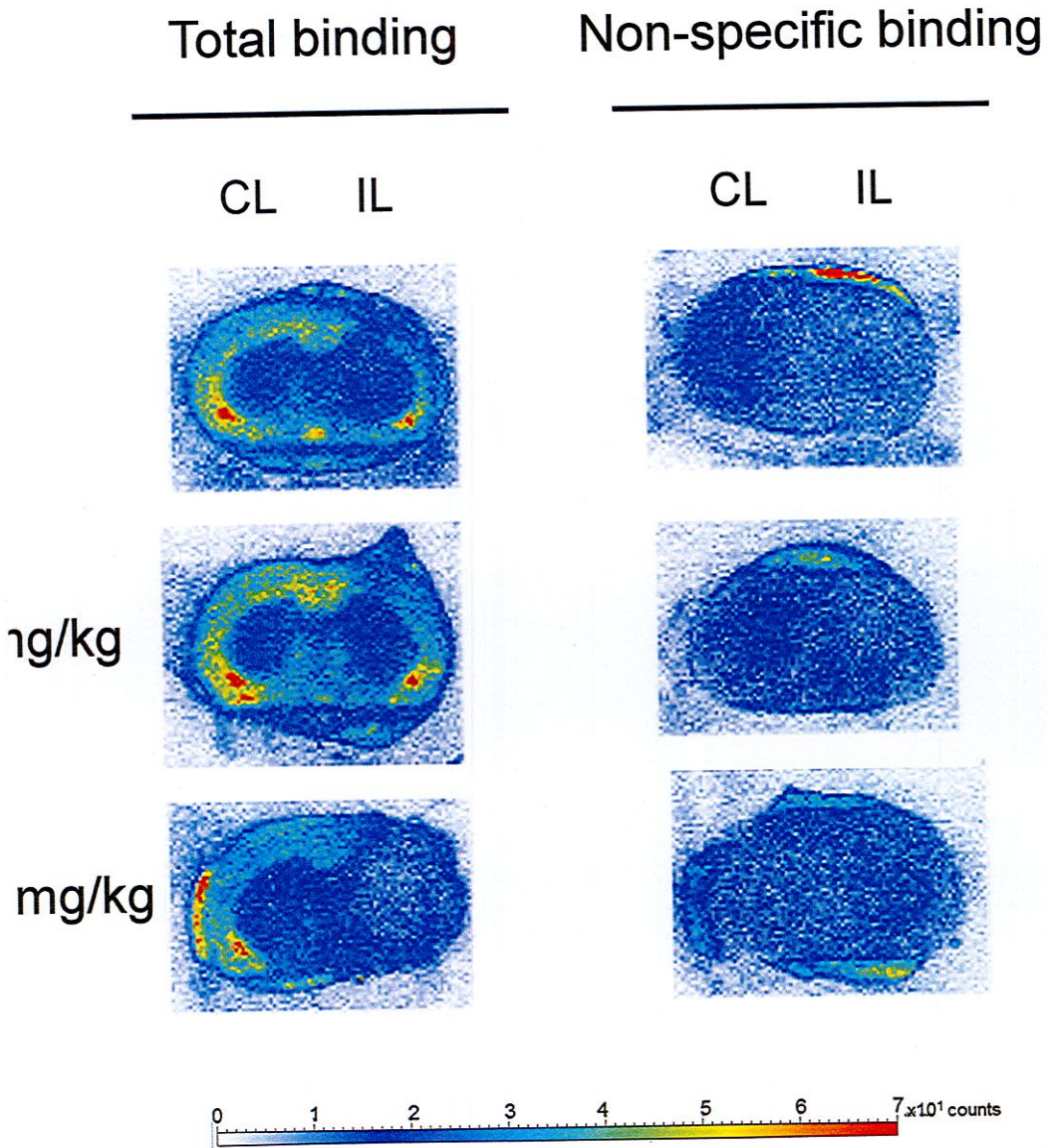
C

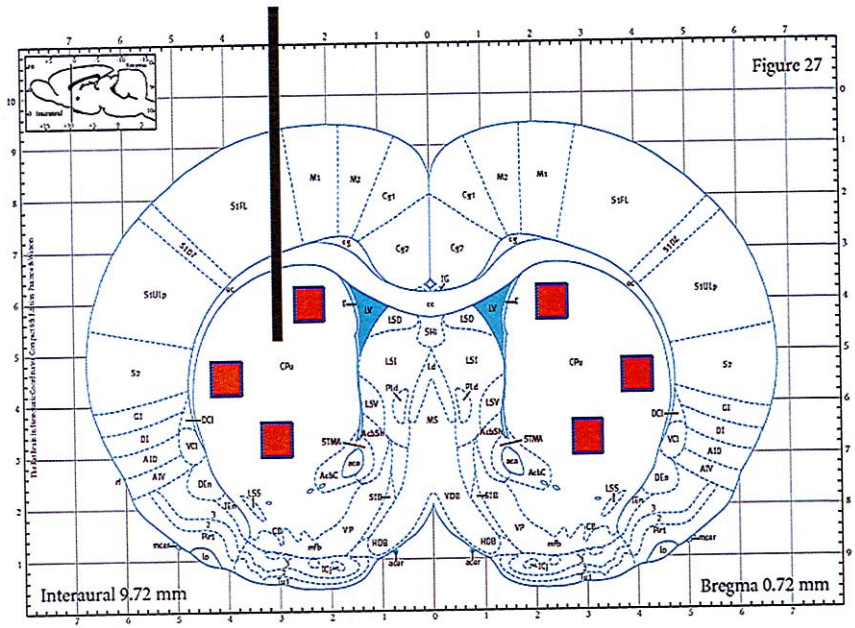




B

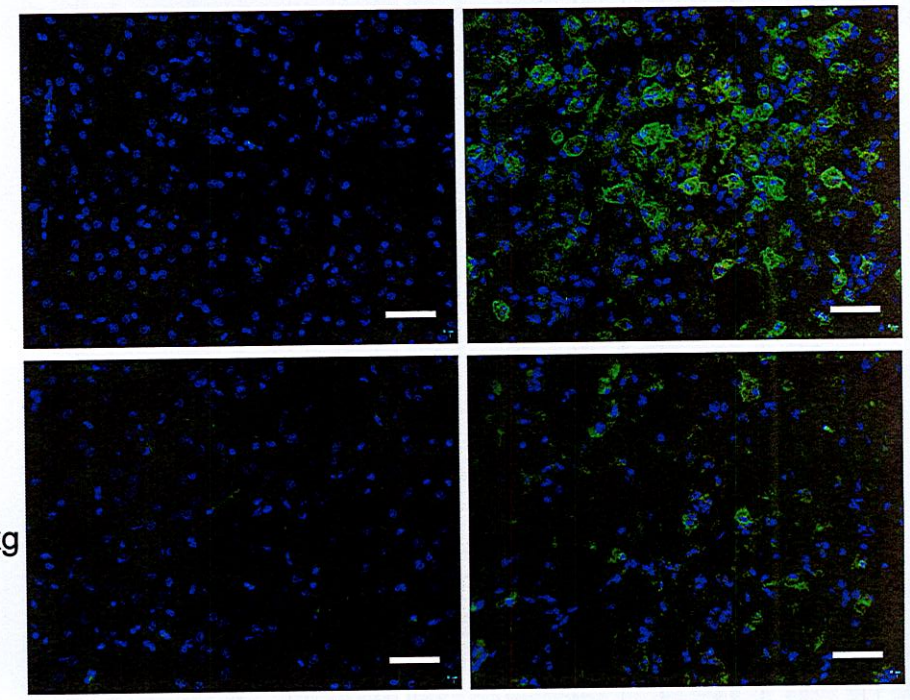


B

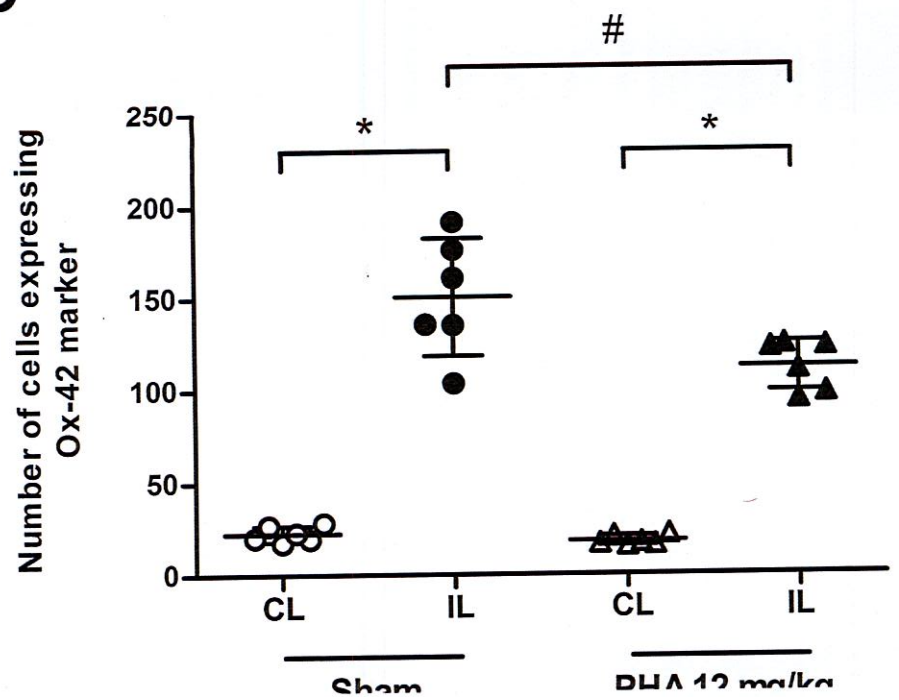


Sham

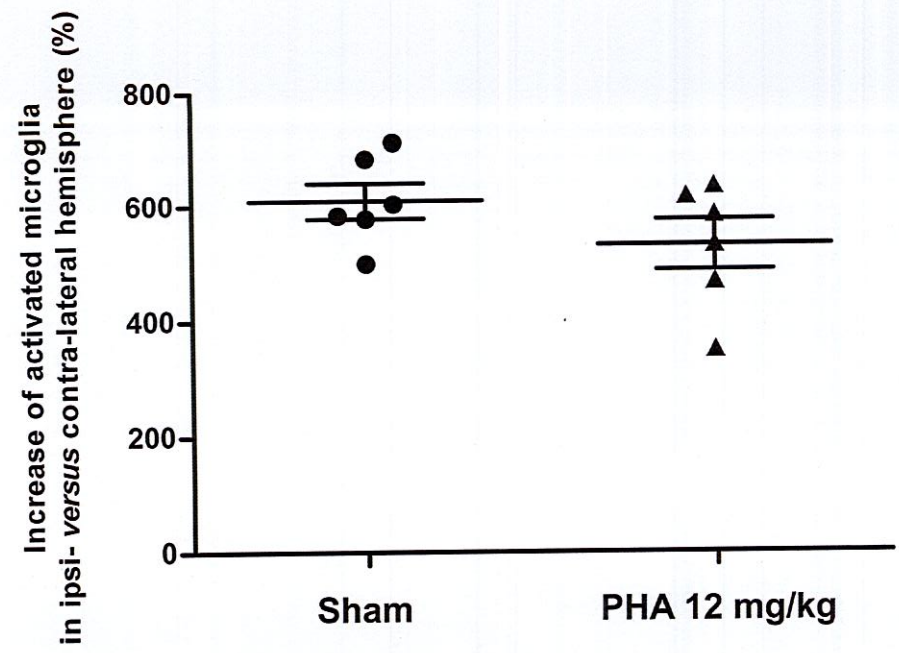
PHA 12 mg/kg

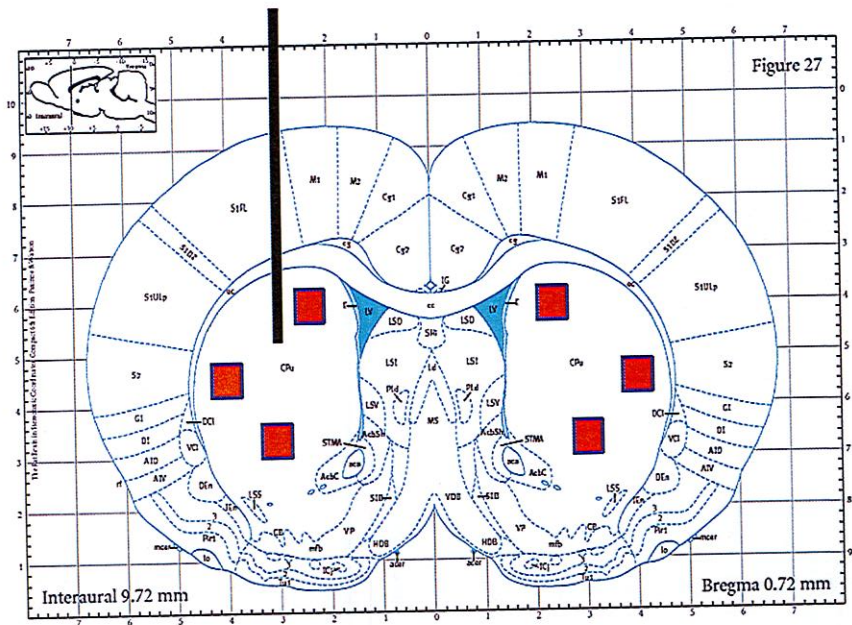


C

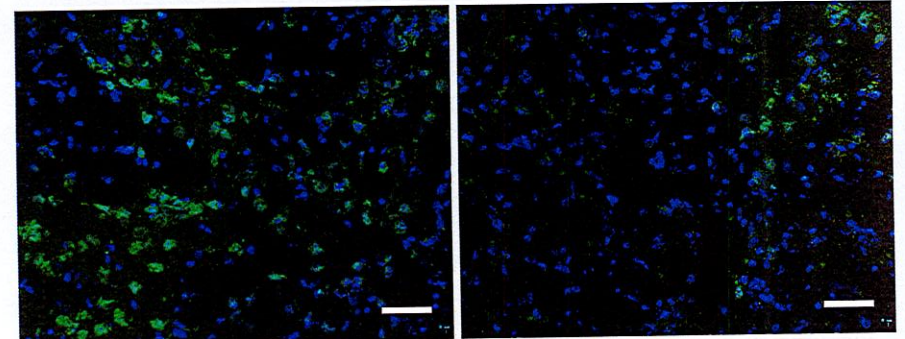


D

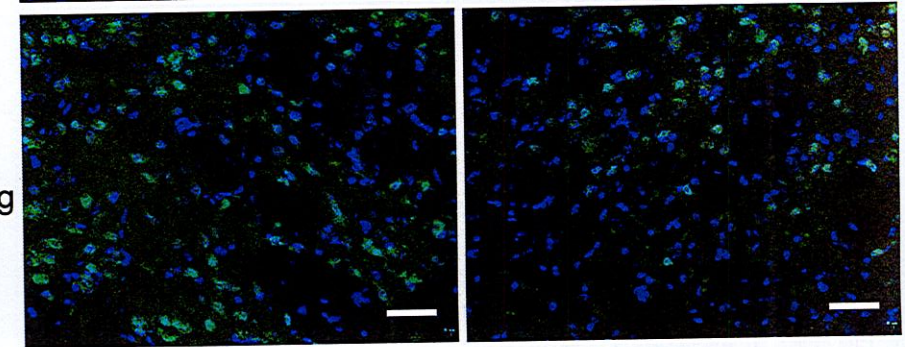




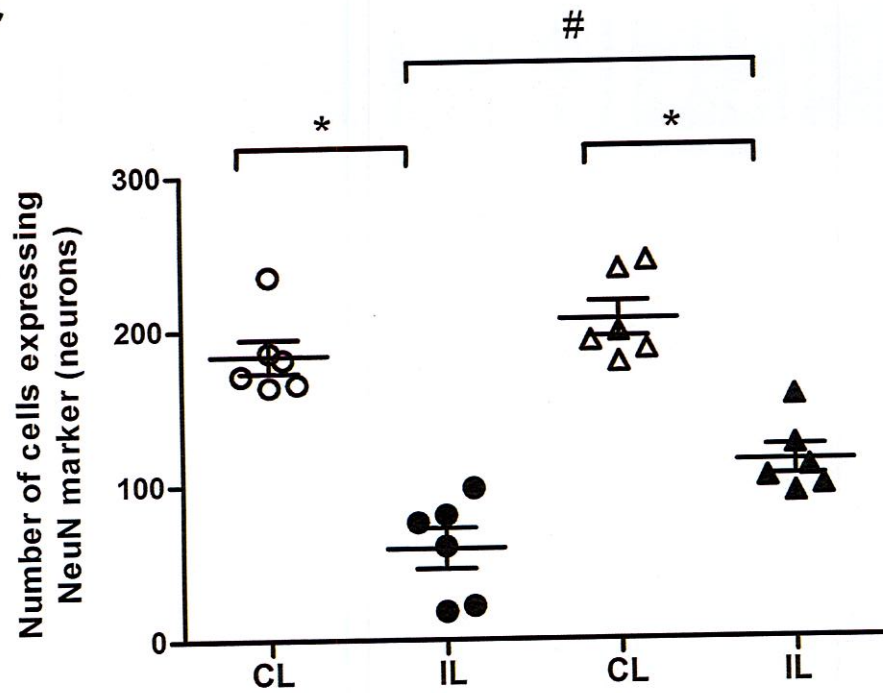
Sham



PHA 12 mg/kg



C



D

